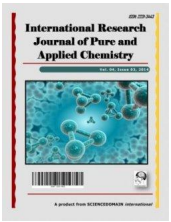

International Research Journal of Pure & Applied Chemistry

15(2): 1-13, 2017; Article no.IRJPAC.37695
ISSN: 2231-3443, NLM ID: 101647669

3D-QSAR Modeling and Molecular Docking Studies on a Series of 1,2,4 Triazole Containing Diarylpyrazolyl Carboxamide as CB1 Cannabinoid Receptor Ligand

Adib Ghaleb[1*], Adnane Aouidate[1], Mounir Ghamali[1], Abdelouahid Sbai[1], Mohammed Bouachrine[2] and Tahar Lakhlifi[1]

[1]Faculty of Science, Moulay Ismail University, Meknes, Morocco.
[2]EST, Moulay Ismail University, Meknes, Morocco.

Authors' contributions

This work was carried out in collaboration between all authors. Author AG designed the study, performed the calculations, wrote the protocol and the first draft of the manuscript. Authors AA and MG suggested and proposed new compounds. Authors AS, MB and TL read and approved the final manuscript.

Article Information

DOI: 10.9734/IRJPAC/2017/37695
Editor(s):
(1) Martin Kröger, Professor, Department of Materials, Computational Polymer Physics, Swiss Federal Institute of Technology (ETH Zürich), Switzerland.
Reviewers:
(1) Otávio Augusto Chaves, Universidade Federal Rural do Rio de Janeiro, Brazil.
(2) Khushbu, Punjab Agricultural University, India.
(3) Geetha Ramakrishnan, Sathyabama University, India.
Complete Peer review History: http://www.sciencedomain.org/review-history/22167

Original Research Article

Received 25th October 2017
Accepted 13th November 2017
Published 6th December 2017

ABSTRACT

3D-QSAR (CoMFA and CoMSIA) and Surflex-docking studies were employed on a series of triazole as CB1 cannabinoid receptor ligand as anti-obesity agents. The CoMFA and CoMSIA models using 20 compounds in the training set gave Q^2 values of 0.9 and 0.93, and r^2 values of 0.98 and 0.97, respectively. The adapted alignment method with the suitable parameters resulted in reliable models. The contour maps obtained from CoMFA and CoMSIA models were used to rationalize the key structural requirements responsible for the activity. Surflex-docking studies revealed that the R3 site, the amine on 1,2,4 triazol group, and the carbonyl were significant for binding to the receptor, some essential characteristics were also determined. Based on the results of 3D-QSAR and surflex-

**Corresponding author: E-mail: adib.ghaleb@gmail.com;*

docking, a set of new compounds with high predicted activities were designed. The total scoring of inactive, active and proposed compounds were compared to each and other to determine the high energy affinity.

Keywords: 3D-QSAR; CoMFA; CoMSIA; Surflex-docking; anti-obesity; 1,2,4 triazole.

1. INTRODUCTION

Triazoles are the class of heterocyclic compounds, which are under study since many years [1]. Azoles moieties are an important and frequent insecticidal, agrochemical structure featuring of many biological active compounds such as cytochrome p450 enzyme inhibitors [2], peptide analog inhibitors [3], and 3, 5 disubstituted 1,2,4 triazole derivatives [4-6], as per the reports to show fungicidal, herbicidal, anti-inflammatory, and anticonvulsant [7-12]. Chemistry of 1,2,4 triazole and their derivatives have received considerable attention owing to their synthetic and biological importance. 1,2,4 triazole moiety have incorporated into variety of therapeutically interesting drug candidates including antiviral, antimigraine, antifungal, antianxiety, insecticidal, antimicrobial [13-15], and also as tyrosinase inhibitors [16], cannabinoid receptor antagonist activities [17].

In the present study 1,2,4 triazole ring, attached with diarylpyrazolyl carboxamide shows cannabinoid receptor binding affinity or antiobesity activity through the down-regulation of the endocannabinoid system by the specific blockage of CB1 receptors which could induce body weight reduction [18].

Recently the advancement of computational chemistry led to new challenges of drug discovery. The 3D-QSAR methods along with surflex-docking approaches were employed to explore the structure-activity relationship (SAR) of compounds. Comparative molecular field analysis (CoMFA) [19] and comparative molecular similarity indices analysis (CoMSIA) [20], were performed to predict the activities of these molecules and offered the regions where interactive fields (steric, electrostatic, hydrophobic, hydrogen bond donor and hydrogen bond acceptor fields) may decrease or increase the activity. The core idea of the present study is looking for novel 1,2,4 triazole containing diarylpyrazolyl carboxamide as CB1 Cannabinoid receptor- ligand that would show useful antiobesity activity, relying on those developed models. Surflex-Docking was applied to study the interactions between the inactive, actif and the proposed compounds with CB1 cannabinoid receptor (PDB entry code: **2MZ2**). Total scoring of the stable conformation is calculated to compare the energy affinity of the proposed ligands and the active compound of the series. Furthermore, we design a new 1,2,4 triazole containing diarylpyrazolyl carboxamide derivatives by utilizing the structure information obtained from the CoMFA and CoMSIA models, which exhibit excellent predictive potencies.

2. MATERIALS AND METHODS

A database of 26 compounds obtained from literature [21] consisted of 1,2,4 triazole containing diarylpyrazolyl carboxamide as CB1 cannabinoid receptor-ligand as anti-obesity agents, the data set was split into two sets, 20 compounds were selected as training set and 6 compounds were selected as test set, based on a random selection to evaluate the ability of the model obtained. The structures and biological activities of all the training and test set compounds are given in Table 1. This data set used to construct 3D-QSAR (CoMFA and CoMSIA) model and to analyze their physicochemical properties. The IC_{50} values were converted to pIC_{50}, used as dependent variable in the QSAR study, according to the formula described in equation 1.

$$pIC_{50} = - \log IC_{50} \quad (1)$$

Three-dimensional structure building and all modeling were performed using the Sybyl 2.0 program package.

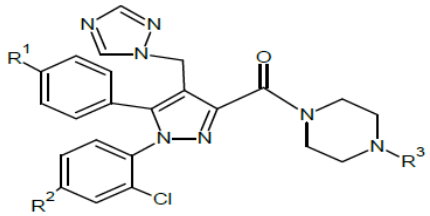

Fig. 1. Chemical structure of the studied compounds

Table 1. Chemical structures and anti-obesity activities of 1,2,4 triazole containing diarylpyrazolyl carboxamide derivatives

No	Structure			pIC_{50}
	R_1	R_2	R_3	
1**	H	H	H	8.34
2	Cl	Cl	Me	5.84
3	Cl	Cl	Phenyl	8.05
4*	Cl	Cl	3-Chloro phenyl	8.05
5	Cl	Cl	2,3-dichloro phenyl	8.26
6	Cl	Cl	2,3-dimethyl phenyl	7.94
7*	Cl	Cl	2-pyrimidyl	7.25
8	Cl	H	Methyl	6.02
9	Cl	H	Ethyl	5.98
10	Cl	H	Phenyl	7.94
11	Cl	H	3-Chlorophenyl	8.39
12	Cl	H	2-3-Dimethylphenyl	8.22
13	Br	Cl	Methyl	5.87
14	Br	Cl	Ethyl	6.55
15	Br	Cl	Phenyl	7.90
16	Br	Cl	3-chlorophenyl	8.14
17	Br	Cl	2,3-Dichlorophenyl	8.24
18	Br	Cl	2,3-Dimethylphenyl	8.42
19*	Br	Cl	2-Pyrimidyl	7.56
20	Br	H	Methyl	6.05
21	Br	H	Ethyl	6.52
22	Br	H	Phenyl	8.10
23	Br	H	3-Chlorophenyl	8.64
24	Br	H	2,3-Dichlorophenyl	8.65
25*	Br	H	2,3-Dimethylphenyl	8.68
26*	Br	H	2-Pyrimidyl	7.65

*Test set molecules; **Outlier compound

2.1 Minimization and Alignment

Molecular structures were sketched with sketch module in SYBYL and minimized using Tripos force field [22] with the Gasteiger–Huckel charges [23] and conjugated gradient method, and gradient convergence criteria of 0.01 kcal/mol. Simulated annealing on the energy minimized structures was performed with 20 cycles. All 26 compounds were minimized to get the low energy conformation of each compound. The fragment 1(the core) is the common structure to all 26 compounds that were considered in this study, and the active compound (compound **25**) was used as an alignment template. All molecules were aligned with respect to this fragment, using the simple alignment method in Sybyl [24]. The super imposed structures of aligned data set are shown in Fig. 2.

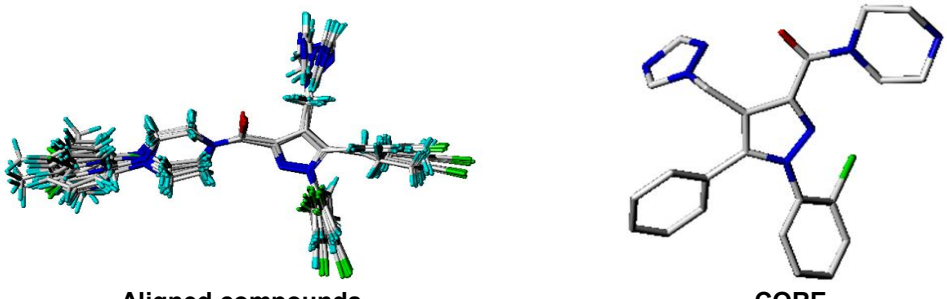

Aligned compounds **CORE**

Fig. 2. 3D-QSAR structure superposition and alignment of training set using molecule 25 as a template

2.2 Outliers

Outliers in the QSAR studies are usually the result of an improper calculation of some molecular descriptors and/or experimental error in determining the property to model. They influence greatly any least square model, and therefore the conclusions about the biological activity of a potential component based on such a model are misleading.

2.3 3D-QSAR Studies

To understand and explore the contributions of electrostatic, hydrophobic and steric fields of the data set and to build predictive 3D-QSAR models based on the molecular alignment strategy.

2.4 CoMFA and CoMSIA

Based on the alignment, CoMSIA and CoMFA studies were used to analyze the specific contributions of steric, electrostatic, and hydrophobic effects. CoMFA calculates electrostatic and steric properties according to Lennard Jones and Coulomb potentials, respectively, whereas CoMSIA calculates the similarity indices in the space surrounding each of the molecules in the dataset. CoMFA steric and electrostatic interaction fields were calculated at each lattice intersection point of a regularly spaced grid of 2.0 A˚. The default value of 30 kcal/mol was set as a maximum steric and electrostatic energy cutoff [25]. With standard options for scaling of variables, the regression analysis was carried out using the full cross-validated partial least squares (PLS) method (leave-one-out) [26]. The minimum sigma (column filtering) was set to 2.0 kcal/mol to improve the signal-to-noise ratio by omitting those lattice points whose energy variation was below this threshold. The final non-cross-validated model was developed using optimal number of components that had both the highest Q^2 value and the smallest value of standard error predictions. The predictive r^2 was used to evaluate the predictive power of the CoMFA model and was based only on test set. Several CoMFA models were built by considering permutations of molecules between training and test sets. The best model amongst them was chosen on the basis of high Q^2, r^2 values and small Standard Error of Estimate (SEE) value. In CoMSIA, a distance-dependent Gaussian-type physicochemical property has been adopted to avoid singularities at the atomic positions and dramatic changes of potential energy for grids being in the proximity of the surface. With the standard parameters and no arbitrary cutoff limits, five fields associated to five physicochemical properties, namely steric (S), electrostatic (E), and hydrophobic effects (H) and hydrogen bond donor (D) and acceptor (A) were calculated. The steric contribution was reflected by the third power of the atomic radii of the atoms. The electrostatic descriptors are derived from atomic partial charges, the hydrophobic fields are derived from atom-based parameters developed by Viswanadhan and the hydrogen bond donor and acceptor indices are obtained by a rule-based method derived from experimental values [27].

2.5 PLS Analysis

Partial least squares statistical method used in deriving the 3D-QSAR models is an extension of multiple regression analysis in which the original variables are replaced by a small set of their linear combinations. PLS method with leave-one-out (LOO) cross-validation was used in this study to determine the optimal numbers of components using cross-validated coefficient Q^2. The external validation of various models was performed using a test set of five molecules. The final analysis (non-cross-validated analysis) was carried out using the optimum number of components obtained from the cross-validation analysis to get correlation coefficient (R^2). The Q^2 value determines the internal predictive ability of the model while R^2 value evaluates the internal consistency of the model. Thus, the best QSAR model was chosen on the basis of a combination of Q^2 and R^2.

2.6 Y-Randomization Test

The obtained models were further validated by the Y-Randomization method. The Y vector (pIC_{50}) is randomly shuffled many times and after every iteration, a new QSAR model is developed. The new QSAR models are expected to have lower Q^2 and r^2 values than those the original models. This technique is carried out to eliminate the possibility of the chance correlation. If higher values of the Q^2 and r^2 are obtained, it means that an acceptable 3D-QSAR can't be generated for this data set because of structural redundancy and chance correlation.

2.7 Molecular Docking

The Surflex-Dock was applied to study molecular docking by using an empirical scoring function and a patented search engine to dock ligands

into a protein's binding site [28]. The crystal structure of CB1 cannabinoid receptor was retrieved from the RCSB Protein Data Bank (PDB entry code: **2MZ2**). The ligands were docked into corresponding protein's binding site by an empirical scoring function and a patented search engine in Surflex-Dock [28]. All water molecules in **2MZ2** have been deleted and the polar hydrogen atoms were added. Protomol, a representation of a ligand making every potential interaction with the binding site, was applied to guide molecular docking.

Protomols could be established by three manners: (1) Automatic: Surflex-Dock finds the largest cavity in the receptor protein; (2) Ligand: a ligand in the same coordinate space as the receptor; (3) Residues: specified residues in the receptor [29,30].

In this paper, the automatic docking was applied. The **2MZ2** structure was utilized in subsequent docking experiments without energy minimization. Other parameters were established by default in the software. Surflex-Dock scores (total scores) were expressed in -log10 (*K*d) units to represent binding affinities. Then, the MOLCAD (Molecular Computer Aided Design) program was employed to visualize the binding mode between the protein and ligand. MOLCAD calculates and exhibits the surfaces of channels and cavities, as well as the separating surface between protein subunits [31–33]. MOLCAD program provides several types to create a molecular surface [28]. The fast Connolly method using a marching cube algorithm to engender the surface was applied in this work, thus the MOLCAD Robbin and Multi-Channel surfaces program exhibited with copious potentials were established. Moreover, Surflex-Dock total scores, which were expressed in –log10 (*K*d) units to represent binding affinities, were applied to estimate the ligand-receptor interactions of newly designed molecules. Each single optimized conformation of each molecule in the data set was energetically minimized employing the Tripos force field and the Powell conjugate gradient algorithm with a convergence criterion of 0.05 kcal/mol A˚ and Gasteiger-Huckel charges.

3. RESULTS AND DISCUSSION

The predicted and experimental activity values and their residual values for both the training and test sets from CoMFA and CoMSIA models are given in Table 2.

3.1 CoMFA Results

PLS summary Table 2 shows that CoMFA model has high R^2 (0.98), F (167.22), and a small S_{cv} (0.137), as well as a great cross-validated correlation coefficient Q^2 (0.90) with four as optimum number of components. The external predictive capability of a QSAR model is generally cross checked and validated using test sets. The five test sets which were selected randomly were optimized and aligned as same as training sets. Moreover, the predicted correlation coefficient r^2_{pred} (0.94) represents that prediction ability of CoMFA model is excellent.

The contributions of steric to electrostatic fields were found to be 90:09, which indicate that the interaction of steric field is extremely important to consider the model have a good quality and predictive capability, and this is in agreement with the hydrophobic character of the cannabinoid ligands.

3.2 CoMSIA Results

Based on CoMSIA descriptors available on SYBYL a 3D-QSAR model was proposed to explain and predict quantitatively the Hydrophobic, Electrostatic, steric, donor and acceptor fields effects of substituents on CB1 cannabinoid receptor ligand as anti-obesity activity of twenty-six 1,2,4 triazole containing diarylpyrazolyl carboxamide compounds.

Different combinations of the five fields were generated. The best CoMISA proposed model contains four fields (Steric, Electrostatic, Hydrophobic, and Acceptor), the cross-validated correlation coefficient Q^2 value of the training set and non-cross-validated correlation coefficient r^2 are 0.93 and 0.97, respectively. The optimal number of principal components using to generate the CoMSIA model is 3, which is reasonable considering the number of molecules used to build the model. The standard error was 0.175. Finally, the prediction ability of the proposed model was confirmed using the external validation, the r^2_{ext} value obtained is 0.97. Those statistics results indicated the very good stability and the powerful predictive ability of CoMSIA model.

3.3 Graphical Interpretation of CoMFA and CoMSIA

CoMFA and CoMSIA contour maps were generated to rationalize the regions in 3D space

around the molecules where changes in each field were predicted to increase or decrease the activity. The CoMFA steric and electrostatic contour maps are shown in Fig. 3. And steric, hydrophobic and hydrogen bond acceptor contour maps of CoMSIA are shown in Fig. 4. using compound **18** as reference structure. All the contours represented the default 80% and 20% level contributions for favored and disfavored regions respectively.

3.3.1 CoMFA contour maps

CoMFA electrostatic interactions are represented by red and blue colored contours while steric interactions are represented by green and yellow colored contours. The bulky substituents are favored in the green regions and at yellow regions, they are unfavored. The blue regions indicate that positive charges are favored, and red regions increase activity only with negative charges.

As Fig. 3a shows, the yellow contour near R1, R2 position indicates that addition of bulky groups would decrease the potency. Whereas the green region around the R3 position indicates, that bulky group is favored, and they might increase the activity. The yellow and green contours can explain very well the discrepancies of Comparing compound **13** (R3=Methyl) with pIC_{50}=5.87 and 25 (R3= 2,3-Dimethylphenyl) with pIC_{50}=8.68.

The red contour near the R2 position indicates that groups with positive charges may increase the activity. This explain why compound **2 (R2=**Cl) with electron-donating substituent at this position is an inactive derivative. A blue contour near the R1 position demonstrated that electron-donating groups would benefit the activity, this explain why compounds **23** (pIC_{50}=8.64), **24** (pIC_{50}=8.65) and **25** (pIC_{50}=8.68) have an electron-donating substituent at R1 (R1=Br) showed significantly increased activities.

3.3.2 CoMSIA contour map

The CoMSIA steric and electrostatic field contour maps were almost like the corresponding CoMFA contour maps.

Table 2. PLS statistics of CoMFA and CoMSIA models

Model	Q^2	r^2	S_{cv}	F-t	N	R_{ext}^2	Fractions				
							Ster	Elec	Acc	Don	Hyd
CoMFA	0.90	0.98	0.137	167.22	4	0,94	0.902	0.098	-	-	-
CoMSIA	0.93	0,97	0.175	149.73	3	0,97	0.367	0.153	0.159	0.00	0.321

Q^2 : Cross-validated correlation coefficient; N : Optimum number of components;
r^2 : Non-cross-validated correlation coefficient; S_{cv} : Standard error of the estimate;
F : F -test value; r_{ext}^2 : External validation correlation coefficient

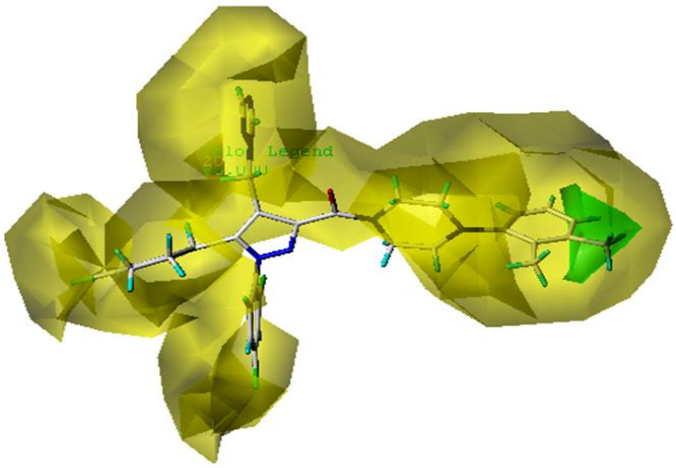

Fig. 3a. Std* coeff. Contour maps of CoMFA analysis with 2 Å grid spacing in combination with compound 18. Steric fields: green contours (80% contribution) indicate regions where bulky groups increase activity, while yellow contours (20% contribution) indicate regions where bulky groups decrease activity

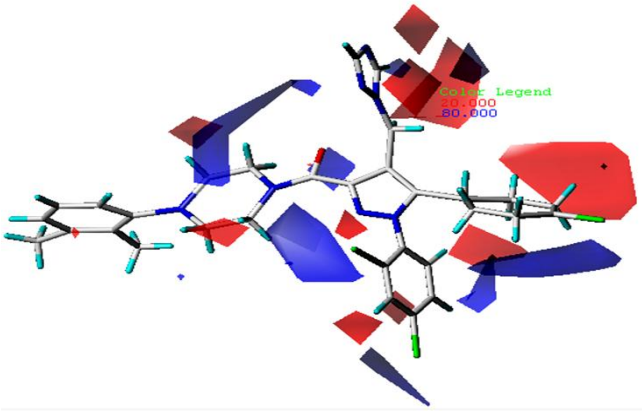

Fig. 3b. Std* coeff. Contour maps of CoMFA analysis with 2 Å grid spacing in combination with compound 18. Electrostatic fields: blue contours (80% contribution) indicate regions where groups with negative charges increase activity, while red contours (20% contribution) indicate regions where groups with positive charges increase activity

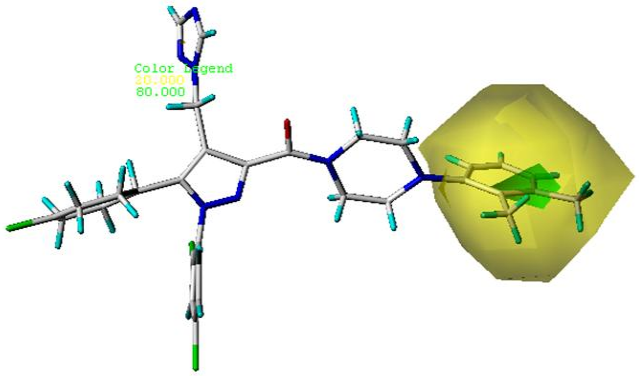

Fig. 4a. Std* coeff. Contour maps of CoMSIA analysis with 2 Å grid spacing in combination with compound 18. Steric fields: green contours (80% contribution) indicate regions where bulky groups increase activity, while yellow contours (20% contribution) indicate regions where bulky groups decrease activity

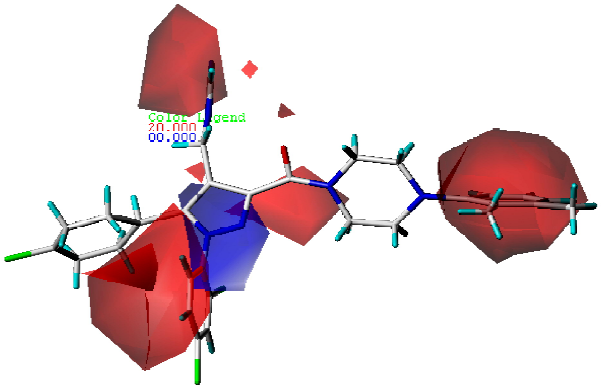

Fig. 4b. Std* coeff. Contour maps of CoMSIA analysis with 2 Å grid spacing in combination with compound 18. Electrostatic fields: blue contours (80% contribution) indicate regions where electron-donating groups increase activity, while red contours (20% contribution) indicate regions where electron-withdrawing groups increase activity

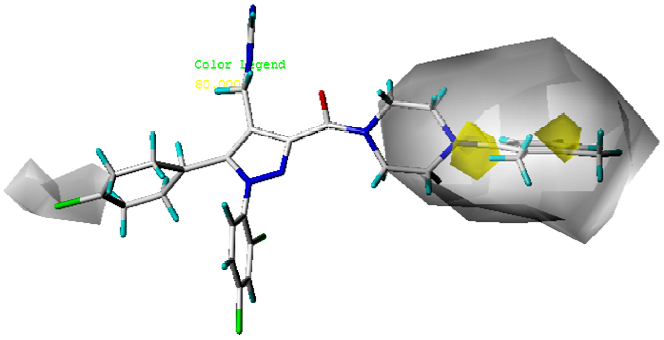

Fig. 4c. Std* coeff. Contour maps of CoMSIA analysis with 2 Å grid spacing in combination with compound 18. Hydrophobic fields: yellow contours (80% contribution) indicate regions where hydrophobic properties were favored, while white contours (20% contribution) indicate regions hydrophilic properties were favored

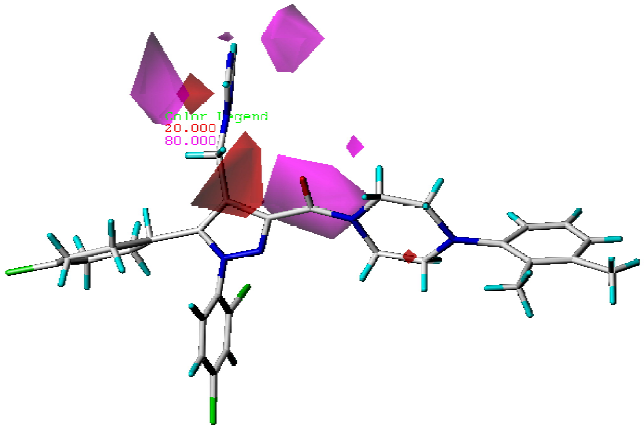

Fig. 4d. Std* coeff. Contour maps of CoMSIA analysis with 2 Å grid spacing in combination with compound 18. H-bond acceptor fields: The purple (80% contribution) and red (20% contribution) contours favorable and unfavorable positions for hydrogen bond acceptors respectively

The two yellow contours around R3 (2,3-Dimethylphenyl) indicate that replacing this position with hydrophilic may decrease the activity. The huge white contour around the piperazine cycle and R1 position indicate that hydrophilic groups are favored.

The purple contour around the carbonyl group revealed a hydrogen bond acceptor substituent at this position would increase the activity. The red contour near N position revealed the importance of the hydrogen bond donor -NH group.

3.4 Y-Randomization

The Y-Randomization method was carried out to validate the CoMFA and CoMSIA models. Several random shuffles of the dependent variable were performed then after every shuffle, a 3D-QSAR was developed and the obtained results are shown in Table 4. The low Q^2 and r^2 values obtained after every shuffle confirmed that the excellent result in our original CoMFA and CoMSIA models are not due to a chance correlation of the training set.

3.5 Design for New Molecules with Anti-obesity Activity

Five new molecules have been designed to enhance the activity, based on the proposed CoMFA and CoMSIA 3D-QSAR models. These compounds were aligned to the database using compound **18** as a template.

Table 3. Experimental and calculated anti-obesity activity (pIC_{50}) with residuals results of compounds in training set and test set for CoMFA and CoMSIA models

Compound no.	Actual pIC_{50}	CoMFA		CoMSIA	
		Predicted pIC_{50}	Residuals	Predicted pIC_{50}	Residuals
2	5.84	5.815	0.025	5.495	0.345
3	8.05	8.013	0.037	8.026	0.024
4*	8.05	7.720	0.330	7.971	0.079
5	8.26	8.353	-0.093	8.164	0.096
6	7.94	8.078	-0.138	7.887	0.053
7*	7.25	7.432	-0.182	7.068	0.182
8	6.02	6.033	-0.013	6.151	-0.131
9	5.98	6.073	-0.093	6.039	-0.059
10	7.94	8.010	-0.070	8.109	-0.169
11	8.39	8.334	0.056	8.196	0.194
12	8.22	8.075	0.145	8.178	0.042
13	5.87	5.740	0.130	5.765	0.105
14	6.55	6.521	0.029	6.802	-0.252
15	7.90	8.018	-0.118	7.949	-0.049
16	8.14	8.143	-0.003	7.981	0.159
17	8.24	8.370	-0.130	8.248	-0.008
18	8.42	8.468	-0.048	8.556	-0.136
19*	7.56	7.982	-0.422	7.815	-0.255
20	6.05	5.953	0.097	6.151	-0.101
21	6.52	6.695	-0.172	7.092	-0.572
22	8.10	8.139	-0.039	8.344	-0.233
23	8.64	8.568	0.072	8.359	0.281
24	8.65	8.701	-0.051	8.356	0.294
25*	8.68	8.114	0.566	8.370	0.310

Table 4. Q^2 and r^2 values after several Y-randomization tests

Iteration	CoMFA		CoMSIA	
	Q^2	r^2	Q^2	r^2
1	0.22	0.92	0.06	0.73
2	0.15	0.60	0.37	0.42
3	0.11	0.80	0.18	0.76
4	-0.60	0.52	-0.15	0.62
5	-0.34	0.84	-0.45	0.72

Table 5. Chemical structure of newly designed molecules and their predicted pIC_{50} based on CoMFA and CoMSIA 3D-QSAR models

No	Structure			*Predicted* pIC_{50}	
	R_1	R_2	R3	CoMFA	CoMSIA
A	I	H	3,5difluoro-4dichloromethylphenyl	9.28	8.37
B	I	H	3,5difluoro-4difluoromethylphenyl	8.98	7.26
C	I	H	4trifluoromethylphenyl	8.85	7.27
D	I	H	2,4,6tribromophenyl	8.69	7.58
E	I	H	5bromo-6chlorophenyl	8.66	8.52

The newly predicted structure A showed higher activity (pIC_{50} = 9.28 and 8.37 for CoMFA and CoMSIA models respectively) than compound **25** (the most active compound of the series).

4. DOCKING ANALYSIS

Surflex-Dock was applied to investigate the binding mode between 1,2,4 triazole containing

diarylpyrazolyl carboxamide (inactive, active and proposed molecules) and **2MZ2** receptor. In this paper, Surflex-Dock could also serve to inspect the stability of 3D-QSAR models established in previous. To visualize secondary structure elements, the MOLCAD Robbin surfaces and Discovery studio visualizer programs were applied. These were used to develop electrostatic potential (EP), H-bond and Hydrophobicity maps, and explore the interaction between the ligand and the receptor also. The proposed active molecule (A) was selected for visualization purposes.

The blue color in Fig. 5 shows hydrophilic character of the ligand, the pink color around R3 group indicate that H-bond donor groups are favored. In Fig. 6, the hydrogen bonding (dashed lines) interactions between the compound **A** (with highest activity) and the key residues (LYS3, ASP4, LEU5, and ARG6) of CB1 cannabinoid receptor (PDB code **2MZ2**) are labeled. A total of four hydrogen bonds were formed: The Fluor at R3 position acted as the hydrogen bond acceptor and formed two H-bonds with the amino group of the ARG6 residue, the carbonyl group on the ligand also acted as the hydrogen bond acceptor and formed H-bond with the amino group of LEU5 residue, the amine on the 1,2,4 triazole groupment acted as H-bond acceptor, and formed H-bond with amino group of LYS3. These results are satisfactorily matched the observation taken from the CoMSIA contour maps.

In Fig. 8, The R3 site was found in a yellow area, which suggested that electron-withdrawing properties would be favored; The observations obtained from this electrostatic potential surface satisfactorily matched the corresponding CoMFA and CoMSIA electrostatic contour maps.

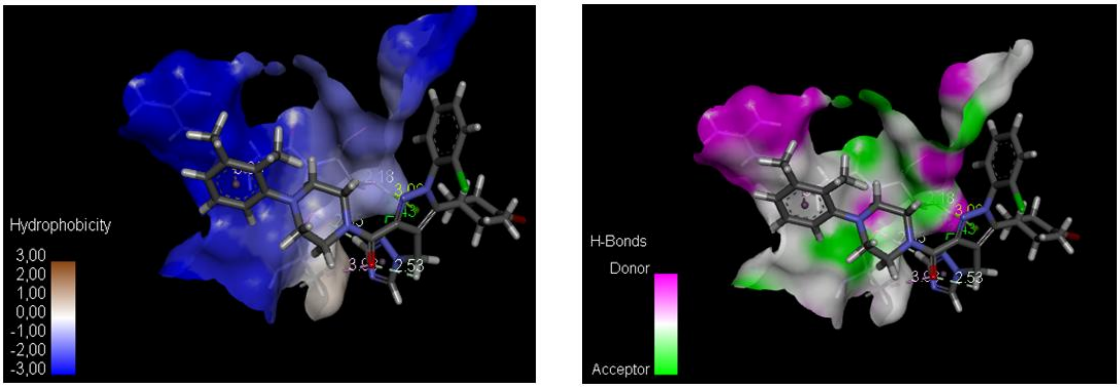

Fig. 5. The interaction H-bond and Hydrophobicity between the active molecule and 2MZ2 receptor, visualized with Discovery studio visualizer program

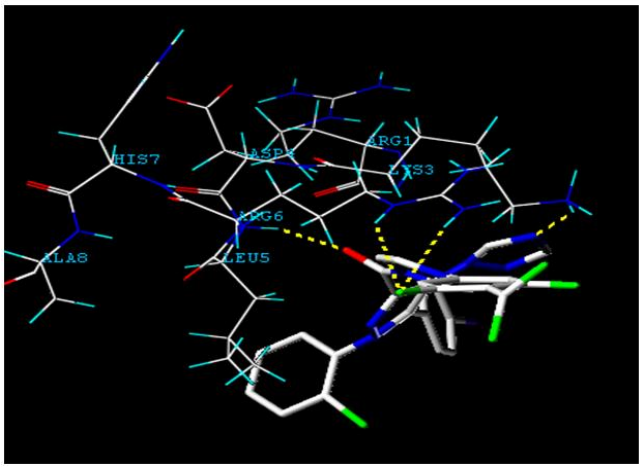

Fig. 6. The binding mode between compound A and the allosteric site of CB1 cannabinoid receptor (PDB code 2MZ2) Key residues and hydrogen bonds are labeled

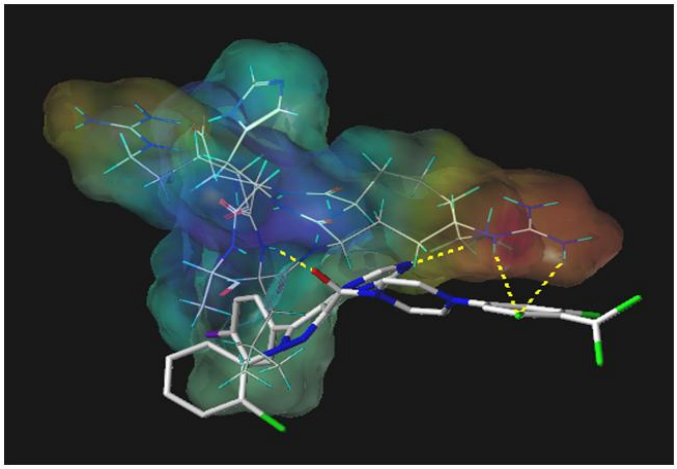

Fig. 7. The MOLCAD electrostatic potential surface of the allosteric site within the compound A. The color ramp for EP ranges from red (most positive) to purple (most negative)

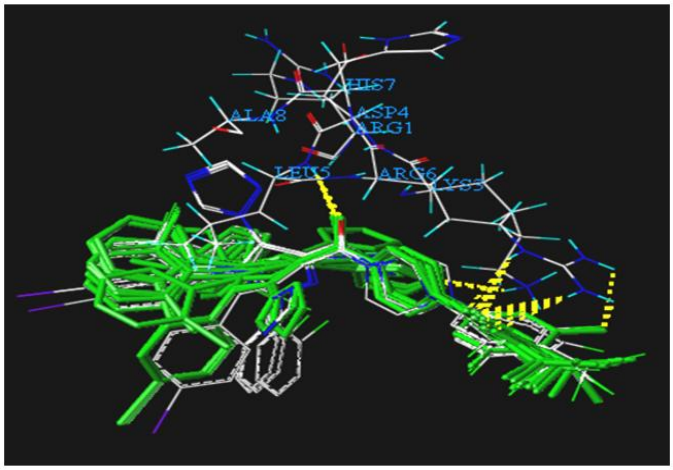

Fig. 8. Overlap of the top-ranked docked poses of compounds A in the active site of CB1 cannabinoid receptor (PDB code 2MZ2)

The surflex-dock total score gives us twenty poses for each molecule, and the stable pose of the inactive structure is the one with a scoring of 1.8, while the active molecule (compound **25**) gives us a scoring with 2.5. The proposed structure (**A**) gives us a stable position with a scoring of 3.25, which indicate that the proposed compound presents an excellent activity compared to those listed in Table 1.

5. CONCLUSION

3D-QSAR and surflex-docking methods were used to explore the structure-activity relationship of series of 1,2,4 triazole as CB1 cannabinoid receptor (anti-obesity). The excellent predictive ability of CoMFA and CoMSIA observed for the test set of compounds indicated that these models could be successfully used to predict the IC_{50} values. Furthermore, the CoMFA and CoMSIA contour maps results offered enough information to understand the structure-activity relationship and identified the structural features influencing the activity. In the present study, a number of novel derivatives were designed by utilizing the structure-activity relationship. Based on the excellent performance of the external validation and total scoring these newly designed molecules can be trustworthy.

ACKNOWLEDGEMENTS

We are grateful to the “Association Marocaine des Chimistes Théoriciens” (AMCT) for its pertinent help concerning the programs.

COMPETING INTERESTS

Authors have declared that no competing interests exist.

REFERENCES

1. Tirlapur KV, Tadmalle T. Synthesis and Insecticidal activity of 1,2,4 – Triazolothiazolidin-4-one derivatives, Pelagia research library -231hgdsa z Der Pharmacia Sinica. 2011;2(1):135-141.
2. Vanden Bossche HJ. Synthesis and insecticidal activity of 1,2,4-triazolederivatives. Steroid Biochem Molec. Biol. 1992;42:45.
3. Meek TD. Peptide aldehydes as inhibitors of HIV protease. J Enzyme Inhib. 1992;6:65.
4. Talawar MB, Laddi UV, Somannavar YS, Benner RS, Bennur SC. Synthesis and antimicrobial activities of some new 1,3,4-oxadiazoles Indian J Heterocycl. Chem. 1995;4:297.
5. Zhang ZY, Yan H. Synthesis and insecticidal activity. Acta Chimicia Sinica. 1987;45:403.
6. Talawar MB, Bennur SC, Kankanwadi SK, Patil PA.Synthesis and pharmacological activities. Indian J. Pharm. Sci. 1995; 57:194.
7. Ramos MG, Bellus D. Synthesis, characterization and biological activity. Angew Chem. 1991;103:1689.
8. Oita S, Uchida T. Ring transformation and complex formation. Jpn Kokai Tokkyo Koho, JP, 10212287. 11August 1998:7.
9. Takao H. 1,2,4 triazole hydrazones. Jpn Kokai Tokkyo Koho JP, 62108868,20 May 1987;11.
10. Shikawa H, Umeda T, Kido Y, Takai N, Yoshizawa H. development of a rice herbicide. Jpn Kokai Tokkyo Koho, JP, 05194432, August 1993:13.
11. Shaker MR. Chemistry of mercapto and thione substituted 1,2,4 triazoles and their utility in heterocyclic synthesis. Arkivoc. 2006;9:59-112.
12. Fotouchi L, Heravi MM, Hekmatshoar R, Rasmi V. Novel electrosynthesis of a condensed thioheterocyclic system containing 1,2,4 triazole ring. Tetrahedron Letters. 2008;49:6628-6630.
13. Jubie S, Sikdar P, Antony S, Kalirajan R, Gowramma B, Gomathy S, Elango K. Synthesis and biological evaluation of some Schiff Bases of [4-(amino)-5-phenyl-4H- 1,2,4- triazole-3-thiol]. Pak. J. Pharm. Sci. 2011;24(2):109-112.
14. Matsumoto O, Uekawa T. synthesis and polymerization. Jpn Kokai Tokkyo Koho JP, 2000239262,5Sep. 2000;13.
15. Nakayama Y, Yano T, production of docosahexenoic acid. Jpn Kokai Tokkyo Koho, JP 03068565, 25 Mar. 1991:9.
16. Nakamura Y., Komatsu H., Yoshihara H, role of c-jun in the inhibition of erythropoietin receptor-mediated. Jpn Kokai Tokkyo Koho, JP 08059675,5 Mar. 1996;5.
17. Ghani U. Ullah N. New potent inhibitors of tyrosinase: Novel clues to binding of 1,3,4-thiadiazole- 2(3H)-thiones,1,3,4-oxadiazole-2(3H)- thiones,4-amino-1,2,4-triazole- 5(4H)-thiones, and substituted hydrazides to the dicopper active site: Bioorg. & Med. Chem. 2010;18:4042-4048.
18. Seo HJ, Kim MJ, Lee SH, Jung ME, Kim MS. Ahn K. Synthesis and structure – activity relationship of 1,2,4-triazole-containing diarylpyrazolyl carboxamide as CB1 cannabinoid receptor-ligand. Bioorg. Med. Chem. 2010;18:1149-1162.
19. Cramer III RD, Patterson DE, Bunnce JD. Comparative molecular field analysis (CoMFA): 1. Effect of shape on binding of steroids to carrier proteins. J. Am. Chem. Soc. 1988;110:5959-5967.
20. Klebe G, Abraham U, Mietzner T. Molecular similarity indices in a comparative analysis (CoMSIA) of drug molecules to correlate and predict their biological activity. J. Med. Chem. 1994;37: 4130-4146.
21. Seo HJ, Kim MJ, Lee SH, Jung ME, Kim MS, Ahn K. Synthesis and structure – activity relationship of 1,2,4-triazole-containing diarylpyrazolyl carboxamide as CB1 cannabinoid receptor-ligand. Bioorg. Med. Chem. 2010;18:1149-1162.
22. Clark M, Cramer RD, Van Opdenbosch N. Validation of the general purpose tripos 5.2 force field. J. Comput. Chem. 1989;10(8): 982–1012.
23. Purcell WP, Singer JA. A brief review and table of semiempirical parameters used in the Hueckel molecular orbital method. J. Chem. Eng. Data. 1967;12(2):235–246.
24. Abdul Hameed MDM, Hamza A, Liu J, Zhan CG. Combined 3D-QSAR modeling and molecular docking study on indolinone derivatives as inhibitors of 3-phosphoinositide-dependent protein

kinase-1. J. Chem. Inf. Model. 2008;48(9): 1760–1772.
25. Ståhle L, Wold S. Multivariate data analysis and experimental design in biomedical research. Prog. Med. Chem. 1988;25:291–338.
26. Bush BL, Nachbar RB Jr. Sample-distance partial least squares: PLS optimized for many variables, with application to CoMFA. J Comput Aided Mol Des. 1993;7:587–619.
27. Viswanadhan VN, Ghose AK, Revankar GR, Robins RK. Atomic physicochemical parameters for three-dimensional structure directed quantitative structure-activity relationships. 4. Additional parameters for hydrophobic and dispersive interactions and their application for an automated superposition of certain naturally occurring nucleoside antibiotics. J Chem Inf Comput Sci. 1989;29:163–172.
28. Sybyl 8.1; Tripos Inc.: St. Louis, MO, USA; 2008. Available:http://www.tripos.com (Accessed on 26 January 2011)
29. Jain AN. Surflex: Fully automatic flexible molecular docking using a molecular Similarity-Based search engine. J. Med. Chem. 2003;46:499–511.
30. Sun JY, Cai SX, Mei H, Li J, Yan N, Wang YQ. Docking and 3D-QSAR study of thiourea analogs as potent inhibitors of influenza virus neuraminidase. J. Mol. Model. 2010;16:1809–1818.
31. Ai Y, Wang ST, Sun PH, Song FJ. Molecular modeling studies of 4,5-dihydro-1hpyrazolo[4,3-h] quinazoline derivatives as potent CDK2/Cyclin A inhibitors using 3D-QSAR and docking. Int. J. Mol. Sci. 2010;11:3705–3724.
32. Lan P, Chen WN, Chen WM. Molecular modeling studies on imidazo[4,5-b]pyridine derivatives as Aurora A kinase inhibitors using 3D-QSAR and docking approaches. Eur. J. Med. Chem. 2011;46:77–94.
33. Lan P, Chen WN, Xiao GK, Sun PH, Chen WM. 3D-QSAR and docking studies on pyrazolo[4,3-h]quinazoline-3-carboxamides as cyclin-dependent kinase 2 (CDK2) inhibitors. Bioorg. Med. Chem. Lett. 2010; 20:6764–6772.

Peer-review history:
The peer review history for this paper can be accessed here:
http://sciencedomain.org/review-history/22167